Direct measurement of ammonia in simulated human breath using an inkjet-printed polyaniline nanoparticle sensor

Troy Hibbard[1], Karl Crowley[1], Anthony J. Killard[1,2*]

[1]Biomedical Diagnostics Institute, National Centre for Sensor Research, Dublin City University, Dublin 9, Ireland;

[2]Centre for Research in Biosciences, Department of Applied Sciences, University of the West of England, Coldharbour Lane, Bristol BS16 1QY, UK

*: E-mail: tony.killard@uwe.ac.uk Tel: +44 117 3282147

Abstract

A sensor fabricated from the inkjet-printed deposition of polyaniline nanoparticles onto a screen-printed silver interdigitated electrode was developed for the detection of ammonia in simulated human breath samples. Impedance analysis showed that exposure to ammonia gas could be measured at 962 Hz at which changes in resistance dominate due to the deprotonation of the polymer film. Sensors required minimal calibration and demonstrated excellent intra-electrode baseline drift (≤ 1.67%). Gases typically present in breath did not interfere with the sensor. Temperature and humidity were shown to have characteristic impedimetric and temporal effects on the sensor that could be distinguished from the response to ammonia. While impedance responses to ammonia could be detected from a single simulated breath, quantification was improved after the cumulative measurement of multiple breaths. The measurement of ammonia after 16 simulated

breaths was linear in the range of 40 to 2,175 ppbv (27 to 1,514 μg/m^3) (r^2=0.9963) with a theoretical limit of detection of 6.2 ppbv (4.1 μg/m^3) (S/N=3).

Key Words

Ammonia, Breath, Impedance, Polyaniline, Nanoparticle, Inkjet

1. Introduction

The provision of real-time, point-of-care diagnostic and analytical information in a non-invasive manner is a major goal of modern biomedical diagnostics. There are several routes to non-invasive or minimally invasive measurements. One extremely attractive route is exhaled breath. Extensive research has shown that links exist between breath gas concentrations and pathologies of the human body. For example, excessive levels of acetone have been shown to correlate with the incidence of diabetes [1], while breath formaldehyde levels have been linked with cancer [2]. Another volatile breath gas of interest is ammonia, and its potential link with dysfunctions of the kidneys and liver [3]. Ammonia is produced as part of the process of nitrogen metabolism and is eventually converted to urea and excreted from the body as part of the urea cycle [4]. Significant quantities of ammonia are also produced by intestinal flora which must also be detoxified by the liver. In instances of liver dysfunction, or in some rare genetic disorders in which ammonia is not metabolised correctly, blood ammonia levels may become elevated. In

some cases, this becomes toxic, leading to hepatic encephalopathy. Here, ammonia crosses the blood-brain barrier, leading to cognitive impairment, coma and, in extreme cases even death [5]. In cases of kidney dysfunction, ammonia, urea and other forms of blood nitrogen such as creatinine are not excreted effectively and these levels rise in blood, while urea is also converted back to ammonia by the gut flora. Current established methods for measuring blood nitrogen levels are invasive, requiring blood sampling. However, it has been well-established that elevation of ammonia concentrations in blood in turn leads to an increase in its rate of gaseous exchange in the lungs and its elevation in exhaled breath [6]. Exhaled human breath consists predominantly of nitrogen, oxygen, carbon dioxide and inert gases,[7] as well as water vapour at a relative humidity (RH) between 91 to 96% [8]. In addition, it can contain in excess of 1,000 volatile compounds, including ammonia [9]. The level of ammonia in human breath has been measured as being between 50 ppbv (where 1 ppbv of ammonia in human breath is approximately 0.67 $\mu g/m^3$) and several thousand ppbv and is dependent on a range of factors including the health status of the patient, the route of sampling (nasal or oral), contribution from oral bacteria, as well as diet, pharmaceutical use and levels of metabolic activity [10]. Thus, the diagnostic measurement of ammonia in human breath must be capable of measuring ammonia in this concentration range, while also being free from interference from other breath constituents. While it is critical to assess the performance of any analytical device in the real sample matrix, the lack of the ready availability of human breath as well as the natural variation of human breath samples leads logically to the use of a source of simulated breath that replicates the major features of natural breath samples with known concentrations of trace ammonia at diagnostically relevant concentrations, while being in constant and convenient availability in the laboratory [11].

A range of methods have been developed for measuring ammonia in human breath [12] and the most successful of these have been instrumental methods such as selective ion flow tube mass spectroscopy (SIFT-MS) and photoacoustic laser spectroscopy (PALS). These systems can directly measure ammonia in human breath down to ppbv levels without interference and in 'real time'. SIFT-MS can also be used to measure a whole host of other volatile trace gases in breath and is an excellent laboratory research tool. However, these systems are large and expensive and are not suitable for translation into application in biomedical diagnostics where 'point of care' type technologies are required.

A number of sensor and microsystems approaches have also been developed for measuring breath ammonia. Timmer *et al.* developed a microfluidic system to measure ammonia using a conductivity sensor [13]. However, the system required the supply of acid and water to sequentially convert the ammonia to ammonium and back to ammonia gas for measurement. In addition, it was only capable of measurement to 1 ppm. Toda *et al.* also demonstrated the measurement of ammonia in breath by dissolving it in a droplet of concentrated sulfuric acid on top of a conductivity sensor and demonstrated low ppb level measurement [14]. However, the nature of the device makes it difficult to fabricate and replicate and lacks robustness for everyday diagnostic use. Finally, Gouma *et al.* developed a MoO_3 based nanosensor which was capable of detecting 50 ppbv ammonia in simulated human breath [15]. However, this required operation of the sensor at 500°C, and even then the signal to noise was very poor preventing quantification at these levels.

The conducting polymer polyaniline has been identified as an ammonia-sensitive material and this mechanism is reasonably well understood. However, briefly, when doped polyaniline interacts with ammonia, the following reaction occurs:

$$PAH^{+}A^{-} + NH^{3} \rightleftharpoons PA + A^{-}NH_4^{+} \qquad (1)$$

where PAH^{+} and PA are the protonated and deprotonated forms of the polymer, respectively and A^{-} is the dopant counter anion [16]. This deprotonation of the polymer backbone leads to a decrease in its conductivity which can be measured in a number of ways. Both Kukla *et al.* [16] and Liu *et al.* [17] observed increases in film resistance for polyaniline films exposed to ppm levels of ammonia. Others have used nanocomposites of polyaniline with multi-wall [18] and single-wall [19] carbon nanotubes and titanium dioxide nanoparticles [20] to achieve ammonia measurement down to as low as 25 ppb. However, their application for measurement in breath has not been illustrated. Aguilar *et al.* demonstrated the use of polyaniline for the detection of ammonia in breath samples using a nanojunction arrangement with electrodeposited polymer and achieved detection of ammonia to 16 ppb [21]. However, the system also required collection of liquid breath condensate in Tedlar bags and its sequential acidification and neutralisation.

Recently, ammonia sensing electrodes using films of inkjet printed polyaniline nanoparticles [22] have been shown to be capable of the measurement of ammonia in air [23] and water [24], with levels of detection down to below 50 ppb using conductance and amperometric techniques. In this work, we demonstrate the application of these

polyaniline nanoparticle electrodes to the measurement of ammonia in artificial breath using impedimetric techniques. We demonstrate that impedance could be used to differentiate between changes in temperature, humidity and ammonia and that breath by breath measurement of ammonia was possible across the full diagnostic range using a simple, disposable sensor.

2. Materials and methods

2.1 Materials

Polyethylene terephthalate (PET) substrates of 175 μm thickness were supplied by HiFi Industrial Film Ltd., (Dublin, Ireland). Electrodag PF-410 silver ink was supplied by Henkel Ireland Ltd. Dodecylbenzene sulfonic acid (DBSA) was purchased from Tokyo Chemical Industry UK Ltd. Ammonium persulfate (APS), aniline (distilled and stored in nitrogen) and sodium dodecyl sulfate (SDS) were purchased from Sigma-Aldrich Co. (Ireland). Oxygen was provided by Air Products Ireland Ltd (Dublin, Ireland). Nitrogen was produced from in-house generators. Carbon dioxide, ammonia, nitric oxide and hydrogen sulfide gases were supplied by Specialty Gases Ltd (Kent, UK). Deionized water (18 MΩ) was from Veolia Water Solutions and Technologies (Ireland).

2.2 Instrumentation

Screen printing was performed on a DEK-248 screen printer (DEK International, UK). Ink-jet printing was performed using a Dimatix DMP 2831 printer with the Dimatix Drop

Manager software (FUJIFILM Dimatix Inc., Santa Clara, CA). Impedance measurements were conducted using a model 660C series electrochemical workstation (CH Instruments Inc., Austin, TX). Simulated breath samples were generated using a combination of respiratory pump and humidifier linked to a microflow controller connected to an ammonia cylinder resulting in a continuous stream of warmed humidified air (62 ±0.67 L/min, 37 ±1°C, ≥90% RH) supplemented with ammonia as appropriate [11]. Ammonia concentrations were calculated from first principles and correlated against photoacoustic laser spectroscopy (Nephrolux, Pranalytica, USA). All gas concentrations were expressed using parts per by volume (ppbv) notation where 1 ppbv ammonia in simulated human breath is equal to approximately 0.67 $\mu g/m^3$.

2.3 Polyaniline nanoparticle synthesis

Polyaniline nanoparticles were fabricated according to Ngamna *et al.* [25] In summary, these were synthesized by adding 3.4 g of 0.25 M DBSA to 40 mL of deionized water. This was stirred at 20°C until the DBSA had fully dissolved. To the DBSA solution, 0.36 g of APS was added and stirred until fully dissolved. This was followed by 0.6 mL of distilled aniline and was allowed to mix for 2.5 hours. After this time, 20 mL of 0.05 M SDS was added to the DBSA/APS/aniline solution which appeared thick and dark green in colour. The DBSA/APS/aniline/SDS solution was then centrifuged at 5,000 rpm for 30 min. The supernatant was transferred to dialysis tubing and dialyzed against 0.05 M SDS for 48 hours. Nanoparticles were characterized by particle sizing and UV-vis spectroscopy. Average particle size was found to be 382 ±33 nm by dynamic light scattering. Spectroscopy displayed peaks at approximately 350, 430 and 765-790 nm,

153 indicating π-π*, π-polaron and localized polaron bands, respectively which was consistent
154 with previous work [25].

155 2.4 Fabrication of sensors

156 Silver interdigitated electrodes were screen printed onto PET using PF-410 cured at
157 120°C for 5 min. A total of ten layers of polyaniline nanoparticle solution were inkjet
158 printed onto the interdigitated electrodes in a circular design of diameter 13.94 mm,
159 covering the entire electrode surface according to Crowley *et al.* [26] The polyaniline
160 nanoparticles were deposited using a 10 pL printer cartridge at 26 V and 5 Khz with a
161 drop spacing of 20 μm using all 16 nozzles.

162 These were allowed to dry in air and then lightly rinsed with deionized water to remove
163 excess SDS. These were dried at 70°C for 30 minutes (Fig. 1). Polyaniline nanoparticle
164 films were examined by scanning electron microscopy and were found to be comparable
165 to electrodes previously fabricated [22].

166

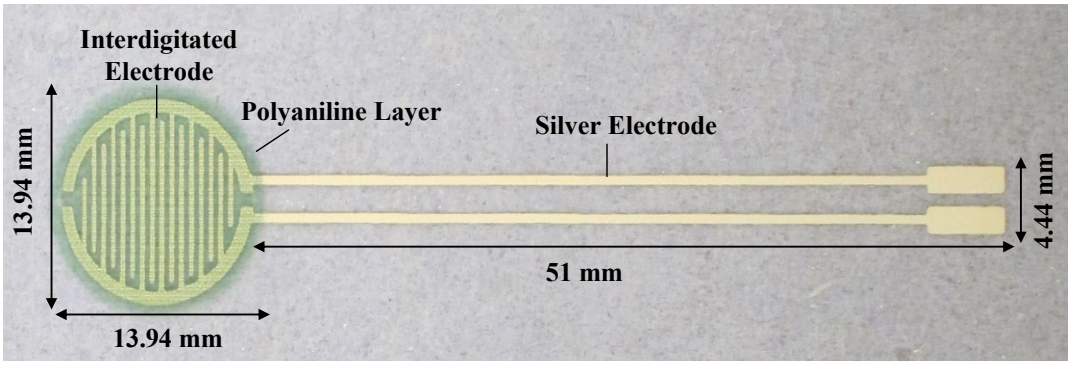

167

Figure 1. Design of the interdigitated polyaniline nanoparticle modified electrode. Screen printed silver interdigitated electrodes were covered with multiple layers of an inkjet printed polyaniline nanoparticle dispersion forming a green film.

2.5 Electrode characterization and analysis of ammonia in simulated breath

The electrochemical impedance characteristics of the electrodes were investigated in the range of 1 Hz to 100 kHz using a 5 mV rms sinusoidal wave form. Sensors were exposed to streams of air, supplemented with concentrations of ammonia at room temperature and 37°C, at ambient and 98% RH or supplemented with other gases. The impedance responses (Z', Z'', |Z| and φ) of the sensors were analyzed. For final breath analysis, changes in |Z| over time were monitored at 962 Hz and a ratio of the absolute impedance at time t (Z) to the background impedance in air (Z_0) [denoted (Z/Z_0)-1] was correlated with ammonia concentration.

3. Results and discussion

3.1 Electrode Impedance Spectroscopic Characterisation

As stated, electrodes formed from polyaniline nanoparticles have been investigated for the measurement of ammonia in air and water using conductimetric and amperometric methods [23,24]. However, neither method was ideal as conductivity measurements require perturbation of the system with a bias potential which can lead to modification and degradation of the polymer film, while amperometric methods do not allow continuous monitoring due to the transient nature of the response, while also requiring a three electrode system and not being suitable for gas phase measurement in a two electrode configuration. Impedance techniques have several advantages in that the

application of a very small perturbation of the system with a small ac signal ensures that the mean film potential is zero. In combination with interdigitated electrodes, it also becomes very sensitive to changes in both the resistance and capacitance of an immobilised layer. When combined with its spectroscopic capabilities, it can also yield significant electrical and electrochemical information on the nature of the film and its interactions. Thus, the polyaniline nanoparticle-modified electrodes were studied with impedance spectroscopy in the 1 Hz to 100 kHz range to evaluate the impact of exposure of the film to ammonia, changes in temperature, humidity and other potential interfering species. Most impedimetric studies of polyaniline-modified electrodes have employed planar electrodes with electrodeposited polymer in solution [27,28]. Some have also used interdigitated electrodes [29,30], but again, the focus has been on solution-phase experiments in which the solution phase becomes a dominant contribution to the electrical model, as opposed to air, which is an insulating dielectric. This work constitutes the first impedimetric analysis of polyaniline nanoparticle films on interdigitated electrodes measured in air.

Bode plot analysis (Fig. 2a) of absolute impedance ($|Z|$) indicated that there was no significant change in the mean $|Z|$ over the range of frequencies in atmospheric air (955 ±1.33 Ω; n=3). However, a noticeable capacitive effect was evident above 962 Hz. This was indicated by a slight decrease in $|Z|$ from 956 to 951 Ω, and a negative change in phase of up to 1.8° at 100 kHz (Fig. 2b). When exposed to ammonia (25 ppmv), the sensors displayed a higher mean $|Z|$ and deviation (2,166 ±17.8 Ω; n=3). As with the results in air, a capacitive component was also evident above 962 Hz. The impedance

decreased from 2,167 to 2,124 Ω, and phase displayed a negative change of up to 2.3° at 100 kHz.

Nyquist plot analysis (Fig. 2c) also presented a relatively simple impedance profile. Measurement in air showed a series resistance of approximately 1 kΩ and a small capacitance of up to 20 Ω that was apparent at frequencies above 967 Hz. Exposure to ammonia resulted in an increase in the offset series resistance to approximately 2,160 Ω and a slightly elevated change in capacitance of 80 Ω at frequencies above 967 Hz. This data is consistent with a simple equivalent circuit model of a resistor and capacitor in series. This increase in resistance due to the addition of ammonia is consistent with the deprotonation of the film. What may seem more surprising is the low capacitance of the film (20 to 80 nF), given that polyaniline has been investigated extensively as a supercapacitor material [31]. However, this may be due to the nature of the films formed from the deposition of the doped polymer nanoparticles which may result in a low surface concentration of charge sites within the polymer, leading to such low capacitances. Based on these findings, further measurements were performed at 962 Hz at which purely resistive changes due to deprotonation of the film by ammonia would be measured. Analysis of $|Z|$ and φ were performed, where appropriate.

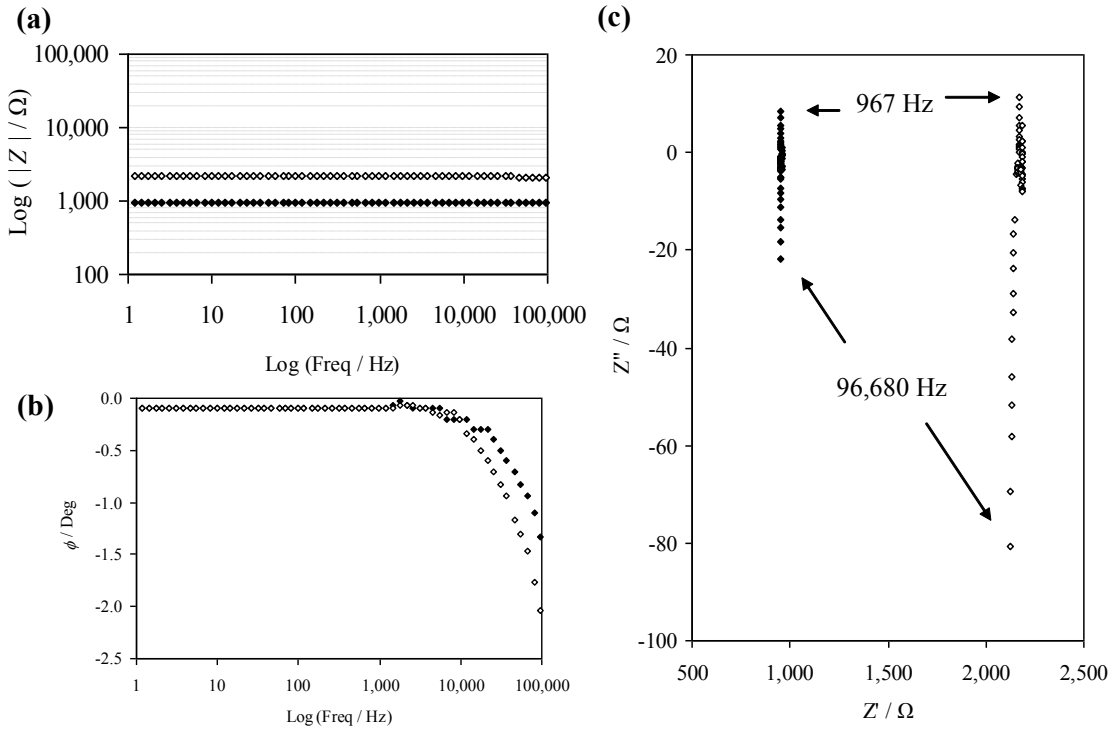

229

230 Figure 2. Impedance and phase behavior of polyaniline nanoparticle-modified electrodes
231 before (filled diamonds) and after (empty diamonds) exposure to 25 ppmv ammonia.
232 Results over the frequency range of 1 Hz to 100 kHz are indicated by (a) Bode, (b) phase
233 and (c) Nyquist plots.

234 3.2 Baseline impedance measurement and ratiometric calibration

235 Baseline stability measurements of the electrodes were performed in air for 600 s with a
236 total of 121 sampling points for each electrode (n=30). The time period of 600 s or 10
237 min. was selected as a suitable time period for the collection of a set of breath
238 measurements. The mean intra-electrode baseline $|Z|$ ranged from 815 to 2,401 Ω with an
239 inter-electrode baseline mean and standard deviation of 1,443.7 Ω and 478.2 Ω (rsd =
240 33%), respectively. Over the 600 s, the intra-electrode drift varied from 1 to 33 Ω (rsd of

241 0.05 to 1.67%). To compensate for the significant inter-electrode variation in baseline and
242 how this might impact on the reproducibility of ammonia measurement, ten electrodes
243 were analyzed ratiometrically based on their initial baseline impedance in air (Z_0)
244 followed by their measurement upon exposure to simulated breath ammonia (Z). Given
245 that breath samples are pulsatile in nature, an experimental methodology was adopted in
246 which simulated breath samples were pulsed across the electrode, followed by a rest
247 period during which the electrode was only exposed to ambient atmosphere. Following
248 establishment of a baseline $|Z|$ in air for 100 s (Z_0), electrodes were repeatedly exposed to
249 4 s pulses of simulated human breath (≥90% RH, 37 ±1°C, 62 ±0.67 L/min) containing
250 ammonia (245 ±8 ppbv), followed by a gap of 15 s for a period of 500 s. Z/Z_0 was
251 determined to be 2.69 ±0.12 (rsd=4.46%, n=10). This deviation of less than 5% suggested
252 that the electrodes could be used without the need for extensive individual calibration
253 other than initial ratiometric baseline correction. Further measurements on the electrodes
254 applied this methodology.

255

256 3.3 Evaluation of the Effect of Interferent Gases

257 A major challenge with sensor-based systems and devices is the lack of selectivity of the
258 sensor materials. Polyaniline is no exception and it can be affected in a number of
259 different ways by many species and to varying degrees [32]. Thus, to ensure that it was fit
260 for purpose for breath ammonia measurement it had to be exposed to both ambient
261 atmospheric gases and gases likely to form a part of the exhaled breath sample. The
262 sensor was tested against carbon dioxide (99% (v/v)), nitrogen (99% v/v), oxygen (99%
263 v/v), hydrogen sulfide (25 ppmv) and nitric oxide (25 ppmv). These concentrations were

264 selected as being well beyond levels that would be experienced in air or breath to over-
265 emphasise any potential interfering effects. The gases were used at room temperature and
266 contained no moisture. Figure 3 shows direct exposure of the electrodes to these gases
267 following exposure to atmospheric air for 300 s. Repeated exposure to concentrations of
268 gas at 0.3 L/min flow rates for 4 s intervals were followed by a rest of 60 s. None of these
269 gases showed any significant impedimetric or phase change responses from the
270 electrodes, all at levels that were well above those that would be realistically found in a
271 human breath sample. However, ammonia (25 ppmv) exhibited an increase in Z/Z_0 with
272 no significant change in phase. This change was consistent with earlier impedimetric
273 analysis and previous literature [33-35]. Analysis of carbon dioxide, nitric oxide and
274 hydrogen sulfide in warmed humidified air showed similar response patterns to those
275 shown, demonstrating no additional contribution from humidity or temperature to the
276 interfering effect of these gases (data no shown).

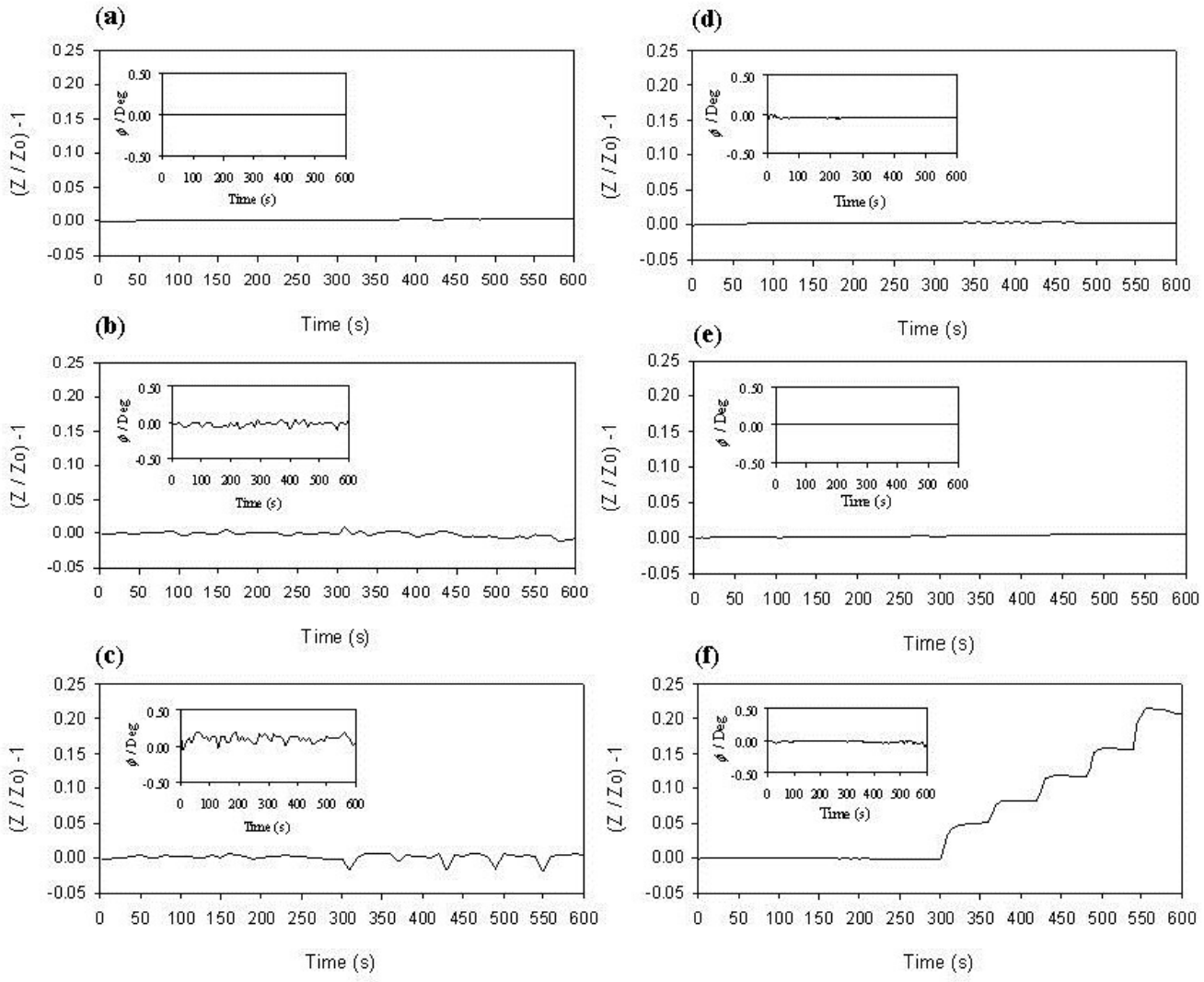

277

278 Figure 3. Ratiometric impedance [(Z/Z_0)-1] and phase (φ) (inset) responses of the
279 polyaniline nanoparticle-modified electrodes to potential interferent gases in human
280 breath: (a) 99% (v/v) carbon dioxide, (b) 99% (v/v) nitrogen, (c) 99% (v/v) oxygen, (d)
281 25 ppmv hydrogen sulfide, (e) 25 ppmv nitric oxide, (f) 25 ppmv ammonia (n=3).

282

283 Polyaniline has been shown to be responsive to CO_2 [36]. However, this has been while
284 in its de-doped, base form whereupon, the carbonate ion acts as a dopant and causes the

285 film to re-protonate. Emeraldine salt forms of the polymer are thus unresponsive to CO_2
286 as observed here as they are already significantly doped, in this case with DBSA. The
287 application of polyaniline base for CO_2 sensing has also been disputed [29].

288

289 A great deal of work has looked at the interaction of oxygen and polyaniline, principally
290 with polyaniline acting as a cathode in the reduction of oxygen. Typically, the onset of
291 oxygen reduction at polyaniline-modified electrodes is -0.4 V [37], and so should not
292 contribute significantly to impedance measurements performed at 0 V, as is the case here.
293 The inert nature of nitrogen also makes it unlikely that it would interact significantly with
294 polyaniline, other than displace other species such as water that may show some effect.
295 However, this was not the case.

296 Work with hydrogen sulfide has shown both significant increases and decreases in
297 conductivity depending on the composition of the polyaniline [26]. The emeraldine salt
298 form of polyaniline has shown weak responses to hydrogen sulfide. However, it was
299 noted that both base-treated polyaniline and copper chloride composite polyaniline
300 displayed significant increases in conductivity. This behavior was similar to the
301 previously discussed base-treated polyaniline and indicated that the polyaniline had been
302 protonated to the salt form. Again, the doped emeraldine form used here also showed no
303 response to hydrogen sulfide, which was consistent with these findings.

304 From this, it was deduced that ammonia was the only major gas in breath that would have
305 a significant effect on the polyaniline nanoparticle-modified electrodes. However, given

306 that real breath contains many more trace volatiles, further studies would be required to
307 show if other gases at diagnostically relevant concentrations might result in interference.

308 3.4 Evaluation of the Effects of Temperature and Humidity

309 Tests were performed to evaluate the effect of atmospheric air at room temperature (21
310 ±1°C), atmospheric air at human breath temperature (37 ±1°C), humidified air at human
311 breath temperature (37 ±1°C, ≥90% RH), and humidified air at human breath temperature
312 containing ammonia (37 ±1°C, ≥90% RH, 245 ±8 ppbv) on the ratiometric impedimetric
313 response of the polyaniline nanoparticle-modified electrodes (Fig. 4). Over a time span of
314 600 s, the first 100 s were again used as the baseline in atmospheric air. Subsequently, the
315 electrodes were exposed to a simulated breath sample for repeated periods of 4 s every
316 100 s.

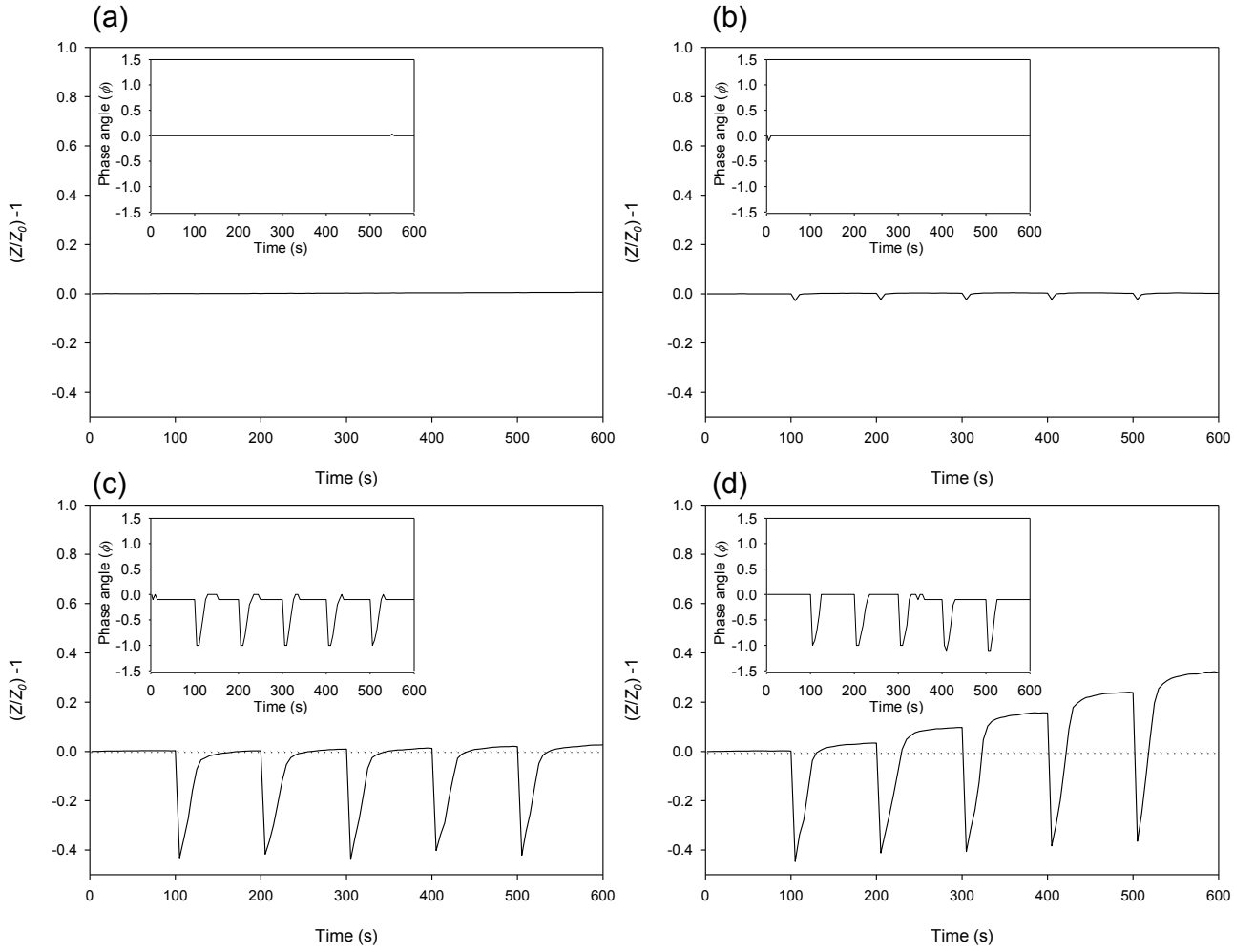

317

318 Figure 4. Polyaniline nanoparticle-modified electrode ratiometric impedance responses
319 [(Z/Z_0)-1], and phase angle (φ) (inset) to (a) room temperature atmospheric air, 21 ±1°C,
320 (b) warmed atmospheric air (37 ±1°C), (c) warmed humidified atmospheric air (37 ±1°C,
321 ≥90% RH) and (d) warmed humidified air with ammonia (37 ±1°C, ≥90% RH, 245 ±8
322 ppbv).

323

324 As might be expected due to the fact that they had already been equilibrated in
325 atmospheric air, the electrodes exposed to a flow of atmospheric air showed no

significant change in ratio-metric impedance, [(Z/Z_0-1)], or φ (Fig. 4a). Atmospheric air warmed to a temperature comparable to that of human breath (Fig. 4b) was detected by the sensor with a very negligible and transient decrease in Z/Z_0, with no observable change in φ. These findings were similar to those seen elsewhere reporting slight changes in conductivity of polyaniline in the range from room temperature to approximately 60°C [23]. When application of the simulated breath sample was removed, the original baseline was rapidly restored as the electrode temperature returned to its original level. However, heated humidified air (Fig. 4c) resulted in a significant transient decrease in Z/Z_0. Furthermore, there was also a noticeable change in phase angle indicating both a change in film resistance and capacitance due to exposure to water vapour. Again, following removal of application of the sample and as the water vapour evaporated from the electrode, $|Z|$ and the φ both returned to their original baselines in a characteristic, time-dependent manner. The effect of temperature and humidity changes on the resistance of polyaniline nanomaterials has been observed elsewhere [38]. In humidified air at human breath temperature containing ammonia (Fig. 4d), the interaction of humidity with the electrodes again caused a negative phase shift and an initial decrease in Z/Z_0, similar to Fig. 4c. However, upon recovery of the electrode from the temperature and humidity effects, an increase in the Z/Z_0 level could be observed, whereas no permanent change in the phase angle was apparent. This suggested that, at this frequency, the ammonia brought about a change in the resistance of the electrodes, whereas water vapour contributed both transient resistive and capacitive effects. This indicated that the impedimetric response signature of ammonia on the electrodes could be differentiated from temperature and humidity components by time-dependent control of the sampling methodology, or

through differential analysis of the changes in impedance and phase. For the present work, a time-controlled breath sampling method was employed.

3.5 Quantification of Ammonia in Simulated Human Breath

The polyaniline nanoparticle-modified electrodes were exposed to 16 sequential simulated breath samples (≥90% RH, 37 ±1°C, 62 ±0.67 L/min) containing ammonia at concentrations from 40 ±2 ppbv to 2,175 ±26 ppbv. Electrodes were repeatedly exposed to 4 s intervals of sample breath gas, followed by a 26 s delay over a 600 s period (Fig. 5).

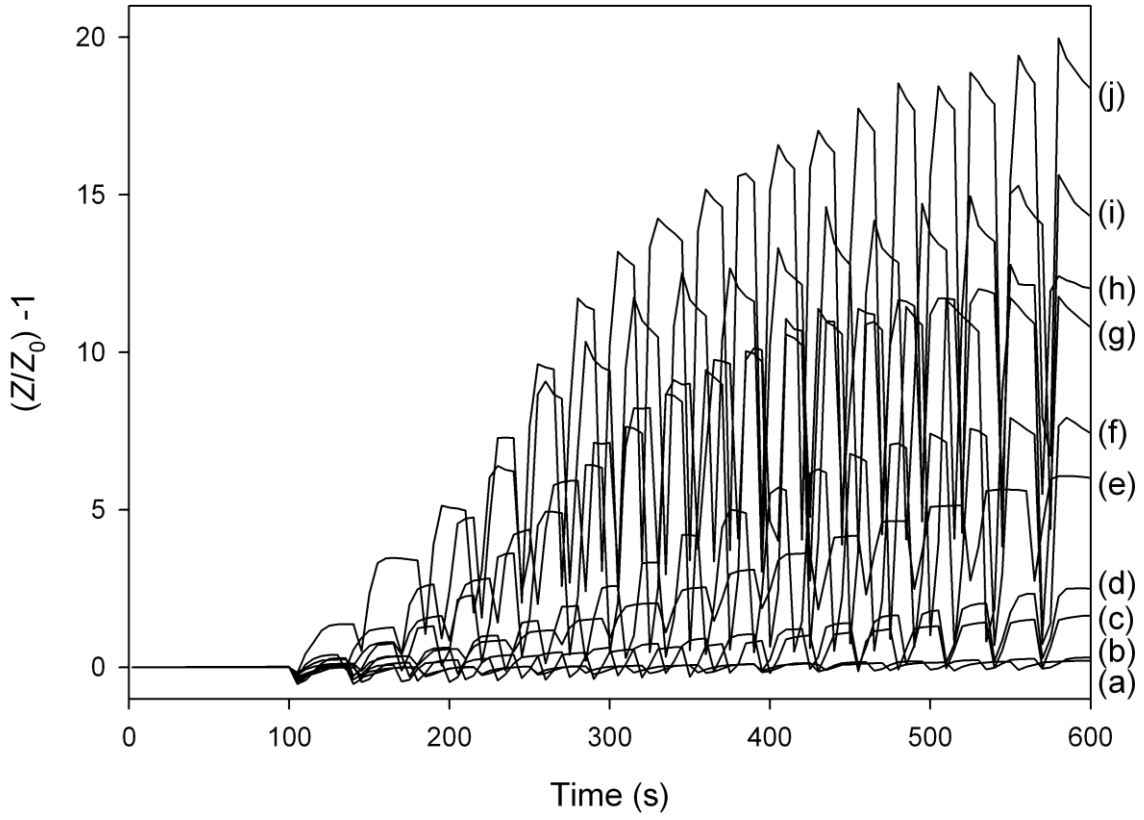

Figure 5. Ratiometric impedance response [(Z/Z_0)-1] profile of simulated breath samples of 4 s duration on polyaniline nanoparticle-modified electrodes measured at 962 Hz. The ammonia concentrations were: (a) 40 ± 2; (b) 121 ±15; (c) 245 ±8; (d) 392 ±6; (e) 755 ±7; (f) 984 ± 21; (g) 1,368 ±11; (h) 1,576 ±7; (i) 1,919 ± 20; and (j) 2,175 ± 26 ppbv.

The characteristic transient decrease in (Z/Z_0)-1 which was shown to be due to temperature and humidity could be observed while the simulated breath sample was being passed over the sensor. In a similar manner to that shown in Fig. 4d, cumulative increases in (Z/Z_0)-1 could be observed for all concentrations of ammonia. It could also be observed that the dissociation of ammonia from the film, as evidenced by the subsequent decrease in (Z/Z_0)-1 becomes more apparent as the concentration increases. Thus, after a specified number of breaths at controlled flow rate (and sample volume), with defined sampling gaps, the change in (Z/Z_0)-1 was proportional to the ammonia concentration.

Peak responses following each simulated breath were averaged (n=3) and plotted to determine the effect of sampling time and the number of cumulative breaths on assay range and linearity (Fig. 6). The changes in Z/Z_0 were observed for each ammonia concentration at every 30 s interval. This showed that the relationship between response and breath number was largely linear for all concentrations until approximately 8 breaths. At higher ammonia concentrations, there was a significant deviation from linearity which is likely to be due to saturation of the polymer with ammonia which may indicate a

progression from surface saturation to bulk saturation. Higher ammonia concentrations also exhibited a greater inter-electrode variability.

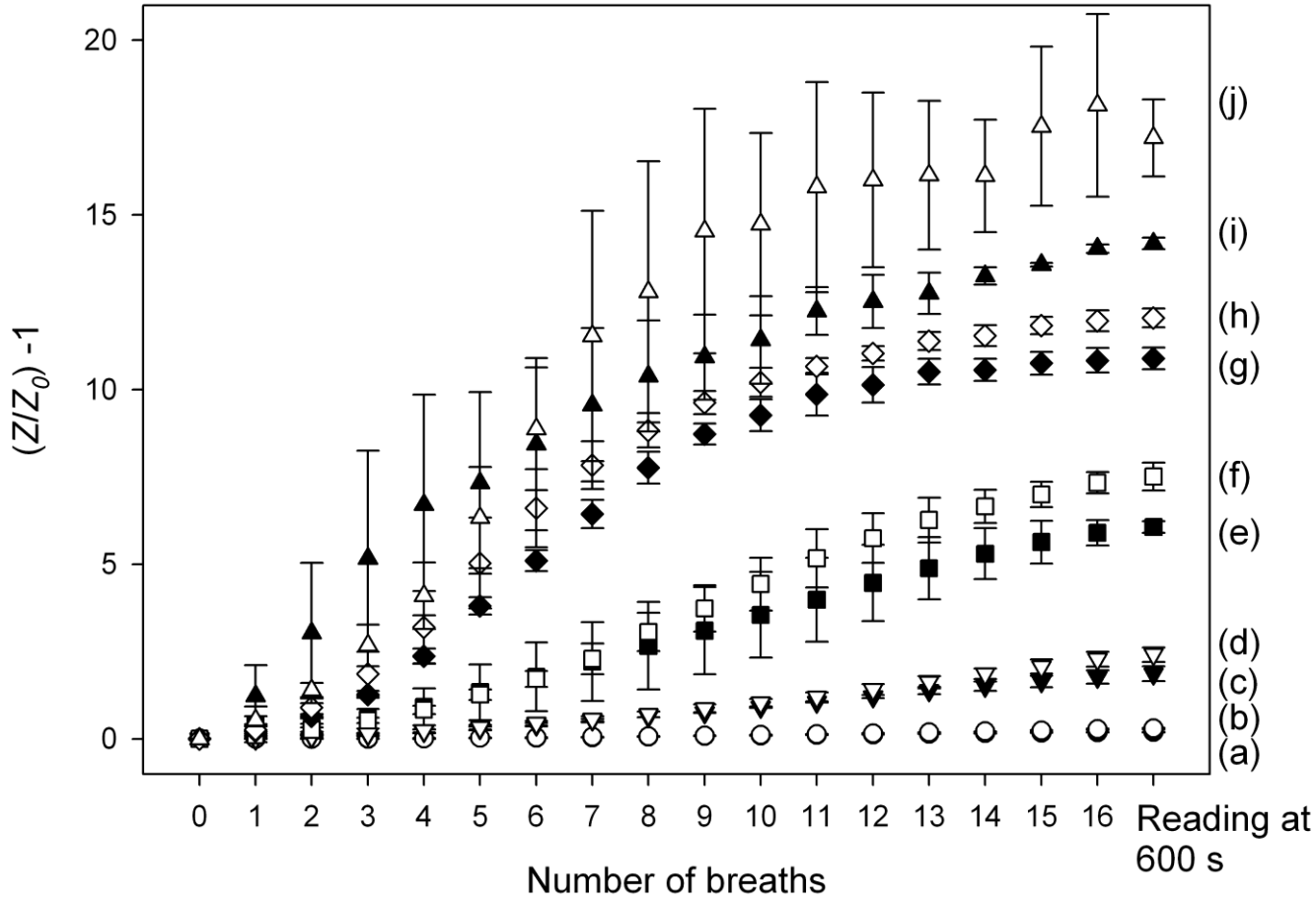

Figure 6. Relationship between ratiometric impedance response and number of cumulative simulated breaths of 4 s duration. Ammonia concentrations were: (a) 40 ± 2; (b) 121 ±15; (c) 245 ±8; (d) 392 ±6; (e) 755 ±7; (f) 984 ± 21; (g) 1,368 ±11; (h) 1,576 ±7; (i) 1,919 ± 20 and; (j) 2,175 ± 26 ppbv.

387 Calibration curves of ammonia concentration vs. impedance response for each number of
388 breaths are shown in Figure 7. The response was found to be linear across the full assay
389 range tested from 40 to 2,175 ppbv ammonia. However, the sensitivity of the response
390 was extremely poor after a single breath measurement. This improved significantly up to
391 approximately 8 breaths at which the polymer film was not yet nearing saturation from
392 ammonia at the higher concentrations. Above this number of breaths, there were no
393 further significant increases in slope. However, the linear regression coefficients between
394 ammonia concentration and Z/Z_0 improved with respect to increased breath number
395 (Table 1). The correlation coefficient was found to be only 0.5584 after a single breath.
396 However, after 16 breaths and measurement at 600 s, this had increased to 0.9963. This
397 increase may be due to the cumulative nature of the sampling methodology as a larger
398 number of samples would average out any sample-to-sample variations, while also
399 benefitting from improved response sensitivity and inherently better signal-to-background
400 ratios.

401

402 A final measurement at 600 s gave a slope and intercept of 0.0079 $ppbv^{-1}$ and -0.3,
403 respectively, and the rsd of the replicates varied between 1.17 and 11.22% (n=3) (Fig. 8).
404 Based on this data in combination with the intra-electrode baseline drift variability
405 determined earlier, a theoretical limit of detection of approximately 6.2 ppbv could be
406 determined (S/N=3) with linearity to 2,175 ppbv ammonia and beyond. This is
407 appropriate for the measurement range required in diagnostic breath measurements of
408 both normal populations and patients with elevated ammonia levels [10].

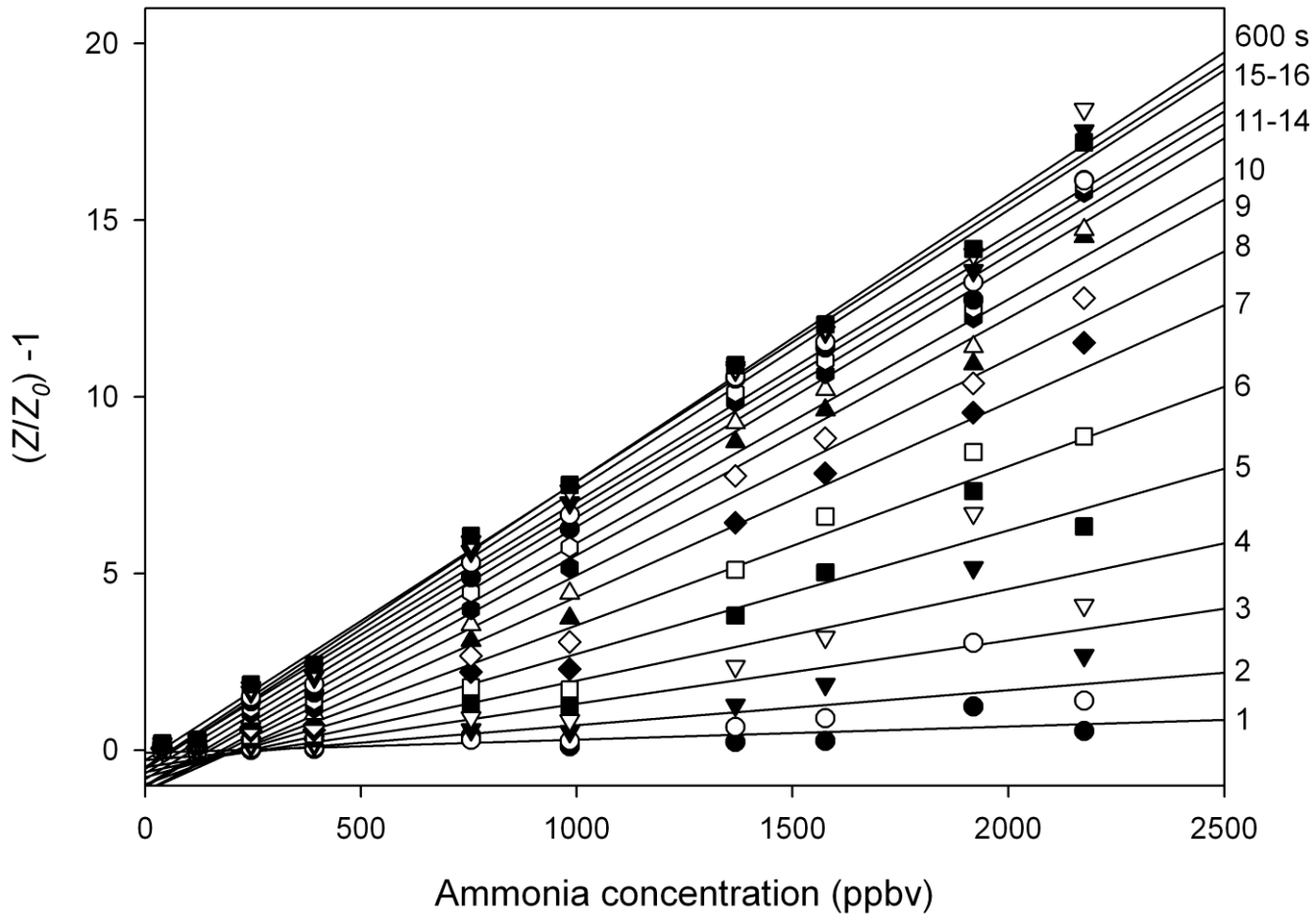

409

410 Figure 7. Relationship between ratiometric impedance response and ammonia
411 concentration with respect to the number of cumulative breaths (1-16) sampled. The value
412 of 600 s indicates a final measurement at this time.

413

414 Table 1. Linear least squares regression coefficients between ratiometric impedance
415 response and simulated breath ammonia concentration with respect to the number of
416 breaths sampled.

Breath Number	Correlation (R^2)	Breath Number	Correlation (R^2)
1	0.5584	9	0.9698
2	0.6475	10	0.9788
3	0.7102	11	0.9837
4	0.8083	12	0.9882
5	0.9257	13	0.9901
6	0.9529	14	0.9942
7	0.9604	15	0.9920
8	0.9694	16	0.9923
		600 s	0.9963

417

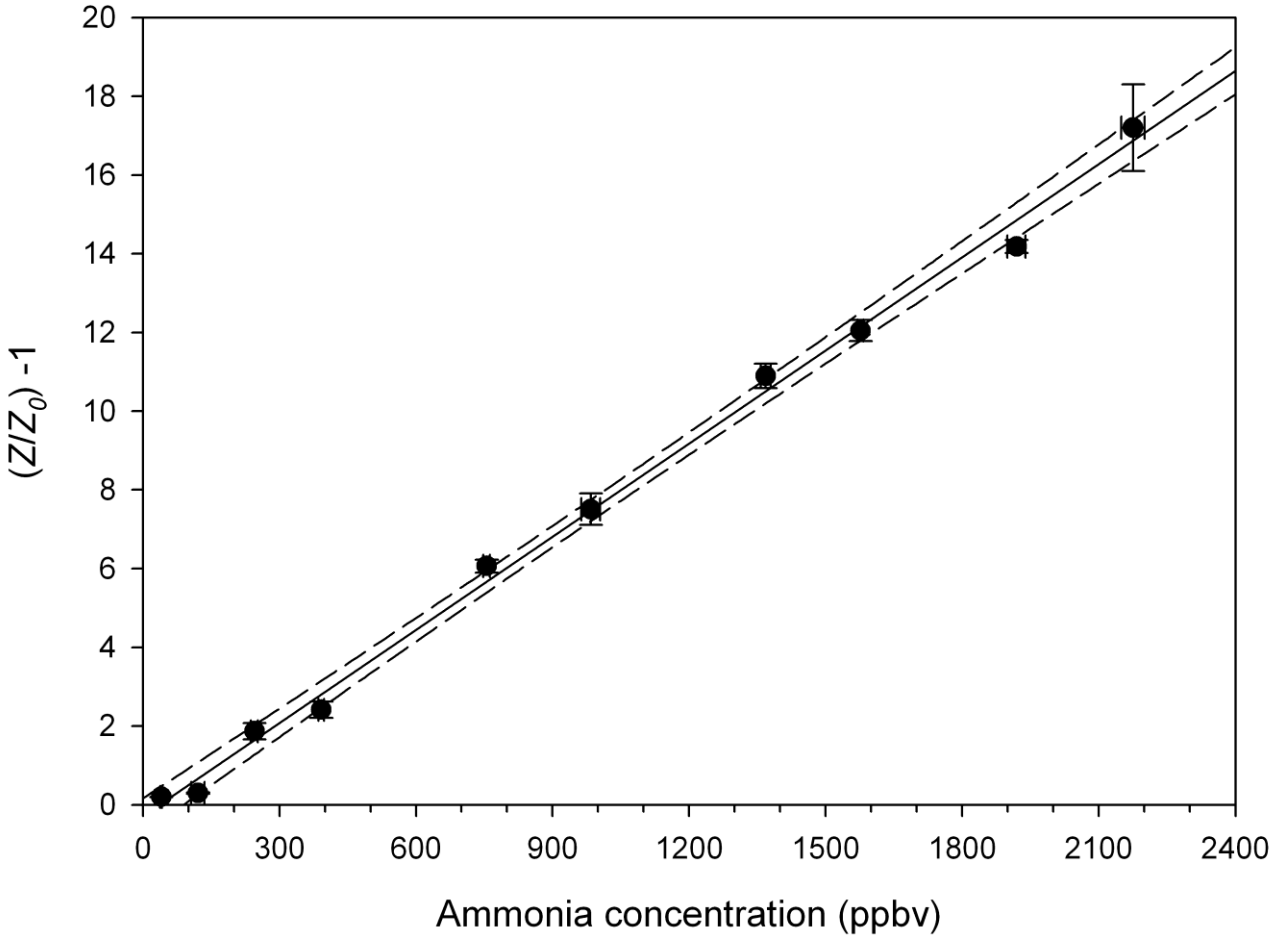

418

419 Figure 8. Relationship between ammonia concentration and ratiometric impedance
420 response after 16 simulated breath samples measured at 600 s (R^2 = 0.9963). A slope and
421 intercept of 0.0079 $ppbv^{-1}$ and -0.2852 were determined. 95% confidence interval (dashed
422 line).

423

424 4. Conclusions

425 An electrode based on an inkjet-printed polyaniline nanoparticle film could be used for
426 the measurement of ammonia in simulated breath. Impedance analysis established a

calibration-free measurement methodology based on ratio-metric measurement of absolute impedance at 962 Hz, 5 mV rms. The sensor was shown to be free of interference from the major gaseous constituents of breath. Effects of temperature and water vapour could also be differentiated from the measurement of ammonia. This allowed the quantitative measurement of ammonia in simulated breath samples across the diagnostically relevant range and demonstrates that these sensors may have potential for measurement of ammonia in human breath for diagnostic applications.

Acknowledgment

This work was supported by Enterprise Ireland under grant number TD/2008/0140.

440 References

441 [1] C.N. Tassopou, D. Barnett, T.R. Fraser, Lancet 1 (1969) 1282-1286.

442 [2] P. Spanel, D. Smith, T.A. Holland, W. Al Singary, J.B. Elder, Rapid Commun. Mass
443 Spec. 13 (1999) 1354-1359.

444 [3] L.R. Narasimhan, W. Goodman, C.K.N. Patel, Proc. Nat. Acad. Sci. USA 98 (2001)
445 4617-4621.

446 [4] J.M. Berg, J.L. Tymoczko, L. Stryer, Biochemistry, fifth ed., W.H. Freeman, New
447 York, 2002.

448 [5] J. Vaquero, R.F. Butterworth, J. Neurochem. 98 (2006) 661-669.

449 [6] H. Wakabayashi, Y. Kuwabara, H. Murata, K. Kobashi, A. Watanabe, Metabol. Brain
450 Dis. 12 (1997) 161-169.

451 [7] G.J. Tortora, Principles of Anatomy and Physiology, elleventh ed., John Wiley &
452 Sons, Inc., New Jersey, 2006, pp. 868-870.

453 [8] G. Zehentbauer, T. Krick, G.A. Reineccius, J. Agri. Food Chem. 48 (2000) 5389-
454 5395.

455 [9] W. Cao, Y. Duan, Crit. Rev. Anal. Chem. 37 (2007) 3-13.

456 [10] T. Hibbard, A.J. Killard, J. Breath Res. 5 (2011) 037101.

457 [11] T. Hibbard, K. Crowley, Z. Shahbazian, A.J. Killard, Anal. Meth. 4 (2012) 2172-
458 2176.

[12] T. Hibbard, A.J. Killard, Crit. Rev. Anal. Chem. 41 (2011) 21-35.

[13] B.H. Timmer, K.M. van Delft, W.W. Koelmans, W. Olthuis, A.van den Berg, IEEE Sens. J. 6 (2006) 829-835.

[14] K. Toda, J. Li, P.K. Dasgupta, Anal. Chem. 78 (2006) 7284-7291.

[15] P. Gouma, K. Kalyanasundaram, X. Yun, M. Stanacevic, L. Wang, IEEE Sens. J. 10 (2010) 49-53.

[16] A.L. Kukla, Y.M. Shirshov, S.A. Piletsky, Sens. Actuat. B 37 (1996) 135-140.

[17] M. Liu, C.L. Dai, C.H. Chan, C.C. Wu, Sensors 9 (2009) 869-880.

[18] Q.F. Chang, K. Zhao, X. Chen, M.Q. Li, J.H. Liu, J. Mater. Sci. 43 (2008) 5861-5866.

[19] T. Zhang, M.B. Nix, B.Y. Yoo, M.A. Deshusses, N.V. Myung, Electroanal. 18 (2006) 1153-1158.

[20] Y.H. Li, J. Gong, G.H. He, Y.L. Deng, Mater. Chem. Phys. 129 (2011) 477-482.

[21] A.D. Aguilar, E.S. Forzani, L.A. Nagahara, I. Amlani, R. Tsui, N.J. Tao, IEEE Sens. J. 8 (2008) 269-273.

[22] A. Morrin, O. Ngamna, E. O'Malley, N. Kent, S. E. Moulten, G.G. Wallace, M.R. Smyth, A.J. Killard, Electrochim. Acta 53 (2008) 5092-5099.

[23] K. Crowley, A. Morrin, A. Hernandez, E. O'Malley, P.G. Whitten, G.G. Wallace, M.R. Smyth, A.J. Killard, Talanta 77 (2008) 710-717.

478 [24] K. Crowley, E. O'Malley, A. Morrin, M.R. Smyth, A.J. Killard, Analyst 133 (2008)
479 391-399.

480 [25] O. Ngamna, A. Morrin, A.J. Killard, M.R. Smyth, G.G. Wallace, Langmuir 23
481 (2007) 8569-8574.

482 [26] K. Crowley, A. Morrin, R. Shepherd, M.I.H. Panhuis, G.G. Wallace, M.R. Smyth,
483 A.J. Killard, IEEE Sens. J. 10 (2010) 1419-1426.

484 [27] A. Sezai Sarac, M. Ates, B. Kilic, Int. J. Electrochem. Sci. 3 (2008) 777-786.

485 [28] V. Horvat-Radosevic, K. Kvastek, Electrochim. Acta 52 (2007) 5377-5391.

486 [29] M. Irimia-Vladu, J.W. Fergus, Synth. Met. 156 (2006) 1401-1407.

487 [30] H. Okamoto, Y. Ando, T. Kotaka, Synth. Met. 96 (1998) 7-17.

488 [31] G.A. Snook, P. Kao, A.S. Best, J. Power Sources 196 (2011) 1-12.

489 [32] U. Lange, N.V. Roznyatouskaya V.M. Mirsky, Anal. Chim. Acta 614 (2008) 1-26.

490 [33] P.P. Sengupta, S. Barik, B. Adhikari, Mater. Manuf. Proc. 21 (2006) 263-270.

491 [34] Z.F. Du, C.C. Li, L.M. Li, H.C. Yu, Y.G. Wang, T.H. Wang, J. Mater. Sci. Mater.
492 Electron. 22 (2011) 418-421.

493 [35] S. Virji, J.X. Huang, R.B. Kaner, B.H. Weiller, Nano Lett. 4 (2004) 491-496.

494 [36] K. Ogura, H.Shiigi, Electrochem. Solid-State Lett. 2 (1999) 478-480.

495 [37] M.M. Gao, F.L. Yang, X.H. Wang, G.Q. Zhang, L.F. Liu, Electroanal. 21 (2009)
496 1035-1040.

497 [38] J. Wang, S. Chan, R.R. Carlson, Y. Luo, G.L. Ge, R.S. Ries, J.R. Heath, H.R. Tseng,
498 Nano Lett. 4 (2004) 1693-1697.